# The application of partial floating end bearing sheet piles to mitigate liquefaction-induced foundation settlements

M. K. Alam
*PhD Candidate, Department of Civil & Environmental Engineering, University of Nevada Reno, Reno, USA*
R. Motamed
*Associate Professor, Department of Civil & Environmental Engineering, University of Nevada Reno, Reno, USA*

**ABSTRACT**

This study investigates the effectiveness of Partial Floating Sheet Piles (PFS) in comparison to full-length sheet piles for mitigating liquefaction-induced settlements in shallow foundations. Although installing sheet piles near foundations is a recognized preventive measure, the high cost of full-length sheet piles has prompted the exploration of alternatives such as PFS. Existing literature lacks comprehensive insights into the behavior and characteristics of PFS. To address this gap, a 1/5 scaled model was utilized, replicating a large-scale shake table test conducted by the University of Nevada, Reno (UNR). The model consisted of three soil layers with varying relative densities, and sheet piles (both full-length and PFS) were strategically inserted using the press-in technique. The research examined PFS variations in the firm layer, covering 50%, 75%, and 87% of the end-bearing segment respectively, to mitigate liquefaction-induced settlements. Results demonstrated that foundation settlement, particularly with PFS at 75% and 87% coverage into the firm layer for fixity of bottom, closely approximated settlements observed with full-length sheet piles. This study provides valuable insights into the potential of PFS as a cost-effective alternative for mitigating liquefaction-induced settlements in shallow foundations.

***Key words:*** *Foundation settlement, Partial floating sheet pile, Soil liquefaction*

## 1. Introduction

Documented case histories of widespread liquefaction have been used to better understand the disastrous impacts of liquefaction-induced foundation settlements. Recent seismic events, notably the 2011 Tohoku Earthquake in Japan, the 2011 Canterbury and Christchurch earthquakes in New Zealand, the 2015 Nepal earthquake, and the 2023 Turkey earthquake (Ashford et al., 2011; Bray & Dashti, 2014; Bai et al., 2017; Cetin et al., 2023), serve as contemporary examples highlighting substantial liquefaction-induced damage to their foundations. One of the major steps in dealing with liquefaction-induced foundation damage is to provide ground improvement techniques to minimize the liquefaction-induced foundation tilt and settlement. The selection of ground improvement techniques depends on various factors, encompassing diverse ground conditions and the intensity of seismic shaking (Motamed & Towhata, 2010). In this study, the effectiveness of sheet piles in mitigating liquefaction-induced foundation settlement is investigated through moderate-scale shake table tests. However, the cost associated with full-length sheet piles can be reduced by implementing partial floating sheet piles (PFS). The PFS method involves the combination of partially floating sheet piles and end-bearing sheet piles (Fujiwara et al., 2020; Kasama, et al., 2020; Otani, 2021).

Harata et al. (2008) studied that the PFS method enabled the decrease of the used weight of sheet piles to approximately half and the total driving length of the PFS method to about 60 percent while studying countermeasures against settlement of embankment on soft ground. In their study, the PFS method had the combination of one end-bearing pile and five floating sheet piles. Fujiwara et al. (2021) carried out numerical analyses using LIQCA3D17, and the test result showed that the end-bearing sheet piles and the floating sheet piles were installed alternately to get the most effective outcome while studying an anti-subsidence countermeasure by the weight of a river embankment built on soft clay ground in a residential area.

However, Harata et al. (2008) and Fujiwara et al. (2021) planned to install partially floating sheet piles in the liquefiable layer, while the end-bearing sheet piles in a stable layer as a countermeasure against liquefaction-induced settlement of embankment on soft ground. However, Rasouli et al. (2015) examined three different configurations of sheet piles, namely continuous, gap, and half-length, to mitigate liquefaction-induced shallow foundation settlement. The investigation revealed that the installation of a gap and half-length is not an effective mitigation in a strong and long shaking. Liquefied sand could easily flow through the gaps between sheets which leads to great settlement of model foundation. To achieve improved performance in reducing liquefaction-induced foundation settlements, it is necessary to use full-length sheet piles that cover the entire liquefiable layer. As a result, our modification involved only changing the end-bearing sheet piles to prepare the PFS.

This study introduces the efficacy of end-bearing PFS into the non-liquefiable layer to mitigate the liquefaction-induced foundation settlement and excess pore water pressure (EPWP) using a series of 1g shaking table tests. In the first step, a scaled ground model was prepared where a shallow foundation was seated over unsaturated soil at the top of the ground model. In the second step, the sheet pile with variable end-bearing length was inserted into the ground model using the press-in technique. A total of five 1g shake table tests were conducted using the same input motions. Finally, conclusions were drawn based on the test results.

## 2. Model properties

### 2.1. Model box

A transparent soil box was utilized with external dimensions of 204 cm in length, 64 cm in width, and 82 cm in height (Toth and Motamed, 2017; Orang et al. 2019; Alam et al., 2023). The container's walls were constructed from 3 cm thick acrylic glass, reinforced with a rigid steel frame. To ensure effective soil saturation and drainage, two drain pipes were installed at the base of the soil box. To minimize boundary effects during dynamic excitation, two high-density foam paddings, each measuring 9 cm in thickness, were inserted on opposing sides of the box. The model box is shown in **Fig. 1**.

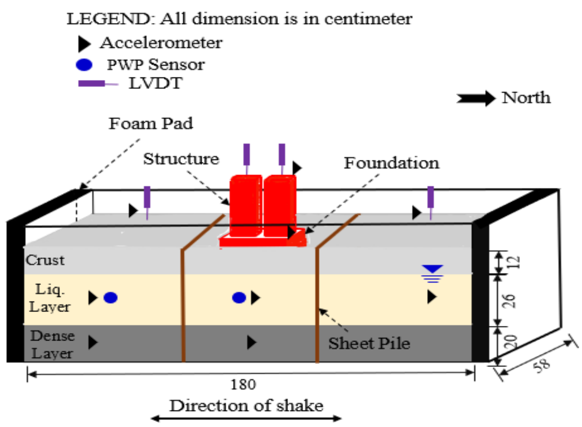


**Fig. 1** Schematic view of the model ground, sheet pile, foundation, and structure

### 2.2. Soil properties

The model ground was constructed using poorly graded #60 Monterey sand, with physical properties of $G_s$=2.65, $e_{max}$ = 0.78, $e_{min}$ = 0.54, $C_c$ = 1.03, $C_u$ = 1.65, and $D_{50}$ = 0.34 (Orang et al. 2019). The ground model consisted of three soil layers with relative densities of 50% for the top crust, 30% for the middle liquefiable layer, and 85% for the bottom dense layer.

### 2.3. Model ground properties

Orang et al. (2021) conducted large-scale shake table experiments at the University of California, San Diego to evaluate the liquefaction-induced settlement of a shallow foundation founded on top of liquefiable ground conditions. The test conducted on a large scale was denominated as the Prototype, while a test of moderate scale conducted within our laboratory was termed the Model. According to the similitude law proposed by Iai (1989), the model ground properties were computed through a large-scale shake table test. A scaling factor of N = 5 was applied, considering the foundation size. Additionally, the input motion parameters, such as peak acceleration and duration, were determined for the model.

The model and prototype properties of the soil thickness, foundation size, superstructure, and input motion are summarized in **Table 1.**

**Table 1.** Properties of the prototype and model based on the similitude law.

| Property | Ratio (Prototype /Model) | Model (N=5) | Prototype (Orang et al. 2021) |
|---|---|---|---|
| Soil layer thickness, (cm) | *N* | 58 | 290 |
| Foundation size (L×W×H), (cm) | *N* | 26×12×8 | 130×60×40 |
| Superstructure load, (kg) | $N^3$ | 26.24 | 3279.47 |
| Peak acceleration, (g) | *1* | 0.53 | 0.53 |

*L=Length, W=Width and H=Height of the foundation*

### 2.4 Model ground preparation

In accordance with the large-scale shake table experiment, the prototype incorporated three distinct soil layers. We adjusted the thickness of these soil layers with relative densities specified as 50% for the upper crust, 30% for the intermediate liquefiable layer, and 85% for the lower dense layer, according to the scaling factor detailed in section 2.3.

Therefore, the dense layer was prepared at first by Monterey sand, where the soil was compacted with 5% moisture content to reach the target relative density of 85%. Subsequently, the compacted dense layer underwent saturation through a gradual percolation of water from the bottom. Following this, the liquefiable layer was created using water pluviation, aiming for a relative density of 30%. A consistent fall height and a water depth of 10 cm were maintained during the pluviation process to facilitate air removal from the falling sand and ensure a 100% degree of saturation. The water table was maintained at the top of the liquefiable soil. Then, the top crust layer was prepared using the air pluviation method, and the foundation was introduced onto the soil model once the crust layer attained a thickness of 4 cm. The final thickness of the crust layer reached approximately 12 cm, with an achieved relative density ($D_r$) of about 50%. After the construction of the soil layer, 26.24 kg weight was mounted on the foundation as a structural load. The model ground is shown in **Fig. 1.**

### 2.5 Sheet pile properties

In this study, Acrylic Premium Sheet (FF) material was used as a sheet pile, and its thickness was determined based on its flexural rigidity, using the similitude law with a scaling factor of 1 (N = 1) (Rasouli et al., 2015). **Table 2** provides specifications of the sheet pile used in the experiment.

**Table 2.** Basic properties of the sheet pile.

| Property | Value |
|---|---|
| Sheet-pile material | Acrylic Premium Sheet |
| Flexural rigidity, (kN-cm$^2$) | 60 |
| Thickness, (cm) | 0.65 |
| Width, (cm) | 56 |
| Distance from the foundation center, (cm) | 16.25 |
| Embedment depth into the ground, (cm) | 58 |

The sheet pile was prepared with the desired dimensions from a large acrylic premium sheet. Then, the 4 pairs of strain gauges were installed using high-strength glue. The placement location of the strain gauge is depicted in **Fig. 2(a).** Before their attachment to the sheet pile, each strain gauge underwent a calibration process. Protective measures were implemented by encasing the gauges in aluminum tape to mitigate potential damage. Additionally, a foam pad was affixed to the side of the sheet pile to facilitate its bending during shaking, as illustrated in **Fig. 2(b).**

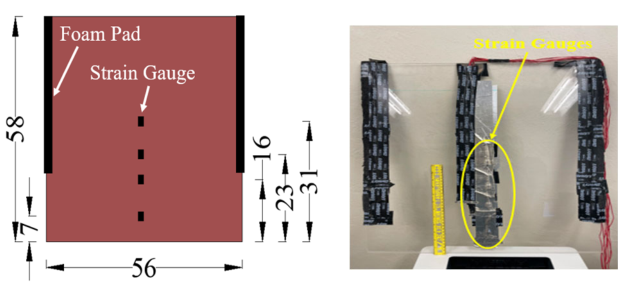


(a) (b)

**Fig. 2** (a) Longitudinal view of sheet pile, (b) Instrumented sheet pile.

In this study, the dense layer was 20cm. Therefore, the full-length sheet pile was embedded 20cm into the dense layer for fixity of the bottom. The embedded portion of the dense layer is named end bearing portion of the sheet pile. The end-bearing portion of the sheet pile was varied to prepare PFS as shown in **Fig. 3.** Three PFS were prepared by cutting 5cm, 10cm, and 20cm respectively. For instance, **Fig. 3(b)** indicates that 5 cm of the end-bearing sheet pile was removed to prepare 5 cm of PFS.

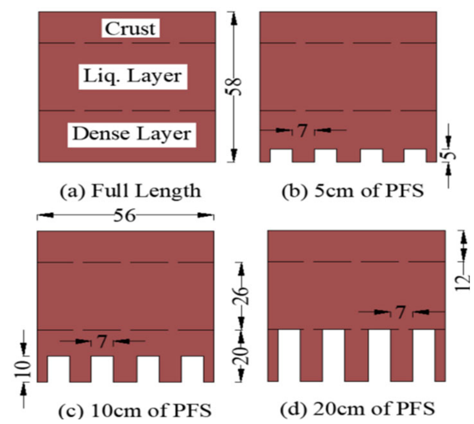


**Fig. 3** Types of PFS adopted in this study

Due to the buckling deformation on the sheet pile, the sheet piles were installed at a pre-defined location before the preparation of the liquefiable layer. Sheet piles were inserted into the model ground by hand pressing at 0.625B (B = foundation width) from the center of the foundation. The placement location of the sheet pile is presented in **Table 2.**

### 2.6 Placement of sensors

A total of 10 accelerometers, 2 pore water pressure, and 4 LVDTs were utilized to measure time histories of acceleration, generation of EPWP, and settlement for both the foundation and the free field. The placement location of the sensors is shown in **Fig. 1.** In addition, two GoPro cameras were also used to record during shaking.

### 2.7 Input motion properties

Though the target acceleration and frequency were 0.53g and 6.68 Hz as shown in **Table 1**, the achieved peak accelerations and frequency of the input motions in the shake table tests were 0.28g and 2.73 Hz. In this study, a 0.28g PGA with a 13s shaking duration was selected due to its ability to provide a comprehensive depiction of EPWP generation and dissipation. Therefore, the duration of the shaking was determined to be 13s, which included a 6s cyclic ramp-up followed by 7s of uniform amplitude motion. To ensure a comprehensive data record encompassing acceleration, EPWP generation and dissipation, as well as foundation settlement, each test was systematically recorded over a total period of 30 seconds. The acceleration time history of the input motion is presented in **Fig 4.**

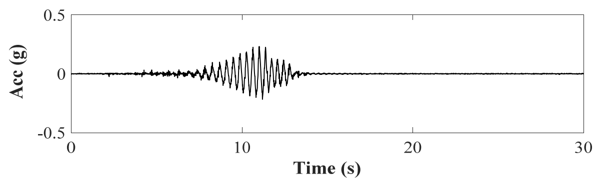


**Fig. 4** Acceleration-time history of input motion.

### 2.8 Test scheme

This study included five 1g shaking table tests. The first shaking table test was carried out on the model ground in the absence of sheet pile installation, and this procedure was designated as the baseline test (referred to as "no mitigation"). Test 2 used full-length sheet piles, while Tests 3 to 5 employed partial floating end-bearing sheet piles. The summary of the test scheme adopted in this study is presented in **Table 3.** The cutting location of PFS (as presented in **Table 3**) is shown in **Fig. 3**.

**Table 3.** The test scheme adopted in this study.

| Test number | Embedment length of end bearing pile (cm) | Floating sheet piles length (cm) | Types of sheet pile | Cutting location of sheet piles |
|---|---|---|---|---|
| FS 1 | - | - | Baseline test | - |
| FS 2 | 58 | - | Full Length | a |
| FS 3 | 58 | 53 | PFS* | b |
| FS 4 | 58 | 48 | PFS | c |
| FS 5 | 58 | 38 | PFS | d |

*PGA=0.28g, Shaking duration= 13s, PFS = Partially Floating Sheet Pile*

## 3. Test results and discussions

The results obtained from 1g shake table tests are presented and discussed in terms of the time history of EPWP generation, and foundation settlement. Then, the visual observation of foundation settlement and titling will be discussed. Finally, the variation of bending moment along the sheet piles will be discussed in the following section.

### 3.1 EPWP time histories

The generation of EPWP during liquefaction is an indication of strength reduction, which can cause liquefaction-induced settlement. Therefore, the PWP sensor was used to monitor the generation and dissipation of EPWP in the shake table tests. The placement of the PWP sensor involved positioning one beneath the foundation and another in the free field both in the middle of the liquefiable layer as depicted in **Fig. 1.** Due to space limitations, EPWP generation underneath the foundation is presented in **Fig. 4**. **Fig. 4** illustrates a wider width of excess PWP generation in the baseline test (FS 1). The incorporation of a sheet pile led to a narrowing of the width of EPWP generation in FS 2. However, in FS 3, a modification was made by cutting the sheet pile by 5 cm, as illustrated in **Fig. 3(b).** The excess PWP generation in FS 3 remained nearly equivalent to that observed in FS 2 because the opening of the end-bearing portion in PFS was only 5cm, therefore the water did not migrate during shaking.

As mentioned in section 2.5, the sheet pile's original length was decreased to 10cm in FS 4, as illustrated in **Fig 3(c),** and reduced to 20cm in FS 5, as shown in **Fig. 3(d).** As depicted in **Fig. 4**, the EPWP in the illustration exhibited a reduced peak and an extended dissipation duration in comparison to FS 2 in **Fig. 4**. This behavior can be explained by the presence of an opening in the end-bearing section of the sheet pile, facilitating the flow of water through the dense layer during shaking.

As depicted in **Fig. 4,** the EPWP generation in FS 5 was less than that in FS 4. This disparity is attributed to the increased height of the opening in FS 5 compared to FS 4. Consequently, the EPWP was able to migrate in and out through the sheet pile, resulting in a lower magnitude of excess PWP but higher dissipation duration during shaking.

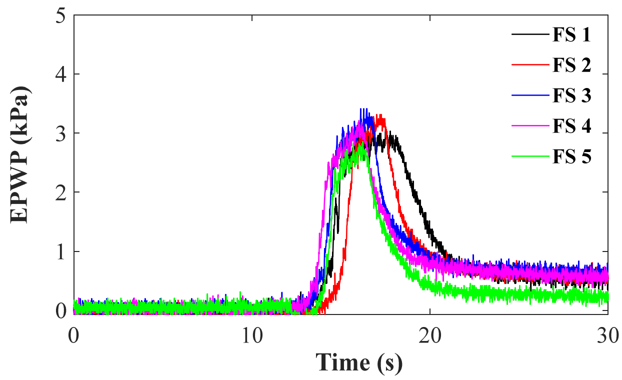


**Fig. 4** EPWP time histories with the application of PFS

### 3.2 Foundation settlement time histories

The LVDT (Linear Variable Differential Transformer) was positioned at the top of the structure to record the time histories of foundation settlement. The specific placement of the LVDT is illustrated in **Fig. 1**, and the corresponding recorded time histories of foundation settlement are displayed in **Fig. 5(a).** Due to space limitations, free field settlement is not presented here. In this study, foundation settlement was assessed by combining settlement from both the shaking and post-shaking phases. In **Fig. 5(a),** the maximum foundation settlement aligned with an increase in EPWP generation. This relationship can be rationalized by the impact of EPWP generation on reducing the shear strength in the underlying soil, resulting in the foundation settlement, and tilting of the structure.

Maximum foundation settlement was calculated from the recorded foundation settlement time histories as shown in **Fig. 5(a).** Then**,** the maximum foundation settlement was plotted against the experiment number as shown in **Fig. 5(b)**. The findings indicate that the implementation of full-length sheet piles led to a greater reduction in foundation settlement when compared to the use of PFS. In addition, the foundation settlement was increasing with the increment of PFS length. As mentioned earlier in Section 3.1, the EPWP was able to migrate in and out through the sheet pile due to PFS, resulting in higher foundation settlement.

To facilitate comprehension, a quantitative analysis of foundation settlement reduction was performed with reference to the baseline test (FS 1). The percentage reduction in foundation settlement is graphically represented against the experiment number in **Fig. 6(a).**

The findings from the tests revealed that both the full-length (FS 2) and "5cm-Cut (FS 3)" configurations of the PFS sheet pile exhibited similar reductions in foundation settlement. As elucidated in section 3.1, the constrained opening in the end-bearing section of the PFS impeded water migration during shaking resulting lower in foundation settlement. As the sheet pile's original length was decreased to 10cm in FS 4, and reduced to 20cm in FS 5, the foundation settlement reduction was decreased. This phenomenon is elucidated by the fact that an increase in the opening of the PFS led to insufficient passive resistance provided by the sheet pile, resulting in an increment of foundation settlement.

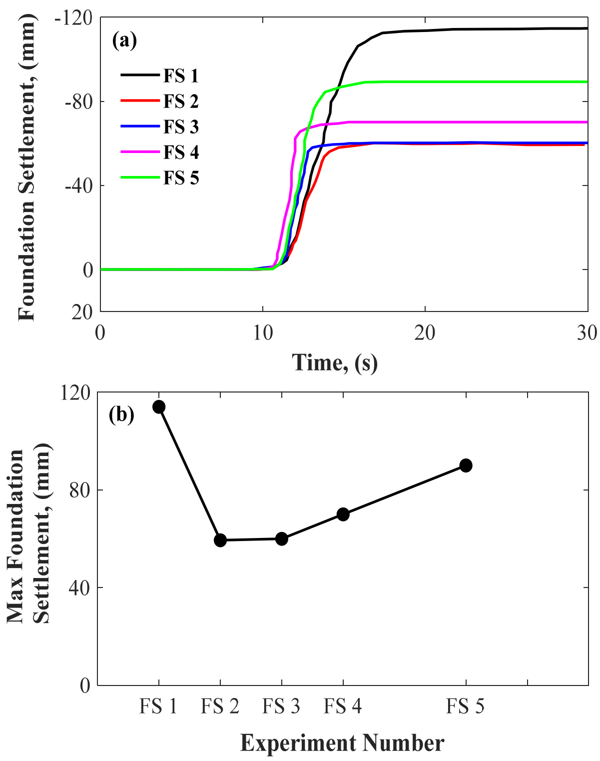


**Fig. 5** (a) Foundation settlement time histories, (b) The variation of maximum foundation settlement with the experimental number.

The reduction in foundation settlement is associated with the coverage of the sheet pile within the dense layer as shown in **Fig. 6(b).** According to calculations, the "5cm-cut (FS 3)" and "10cm-cut (FS 4)" configurations of the PFS could cover 87% and 75% of the dense layer, respectively. Test results indicate that achieving a coverage of 75% or more within the firm layer led to a foundation settlement reduction closely resembling that of a full-length sheet pile. Another investigation focusing on material reduction suggests that covering less area within the firm layer corresponds to a reduction in sheet pile requirements. As mentioned earlier, the "5cm-cut" and "10cm-cut" of PFS contributed to an overall material reduction of 4.3% and 8.75%, respectively.

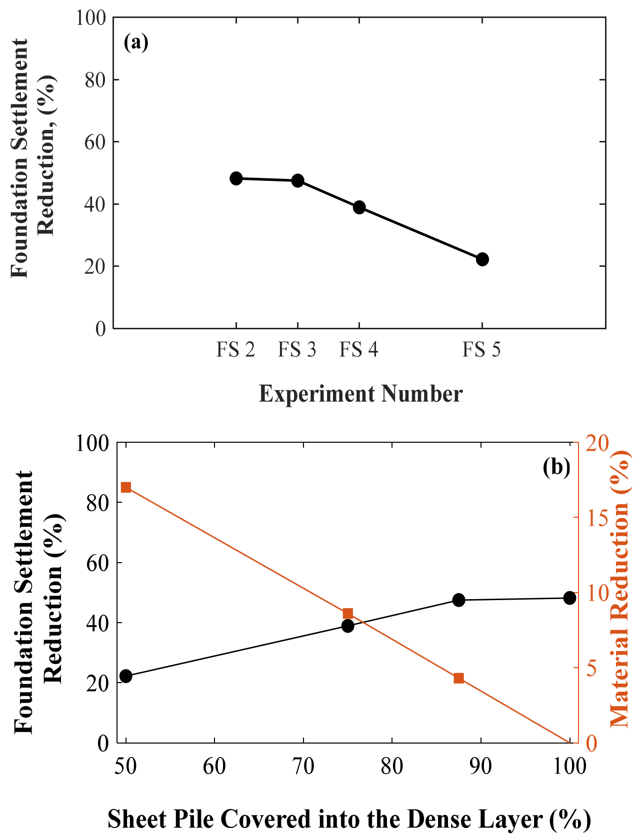


**Fig. 6** (a) The variation of foundation settlement reduction with experimental number, (b) The foundation settlement reduction and material reduction with sheet pile covering into the dense layer

### 3.3 Visual observation on foundation tilting

Foundation tilting is a manifestation of liquefaction-induced damage in shallow foundations and can ultimately lead to the structural failure of buildings in the aftermath of earthquakes. In this study, the initial and post-shaking settlements of the foundation were taken at four corners. The observed settlement alterations at each corner were then used to determine the foundation tilting in both the longitudinal and transverse directions. One limitation of our study is that we did not assess the bearing capacity of the foundation after the shaking occurred.

**Fig. 7** provides an overview of liquefaction-induced foundation settlement observed during various tests. In **Fig. 7(a),** the model ground with the foundation is depicted before the initiation of shaking. As discussed earlier, the baseline test (FS 1) revealed higher levels of foundation settlement and tilting, because of wider width of EPWP generation reduced the effective stress of soil.

Importantly, the application of full-length sheet piles was observed to successfully mitigate longitudinal and transverse directional tilting in FS 2 as shown in Fig. 7(c). In FS 3 and FS 4, both directional tilting of the foundation closely resembled that observed in FS 2, as illustrated in **Fig. 7(d-e)** This indicates that the implementation of PFS in certain openings was effective in mitigating both directional tilting. However, in FS 5, depicted in **Fig. 7(f),** the foundation experienced foundation tilting. This can be explained as the ability of EPWP to migrate in and out through the sheet pile in FS 5. Therefore, the foundation lost stability during shaking resulting in higher foundation tilting compared to other PFS tests. An additional observation was made for FS 5, whereby water emerged onto the surface within the confined area due to the application of PFS with a higher opening, resulting in a loosening of the surface. However, a very limited amount of water was observed in FS 3 and FS 4.

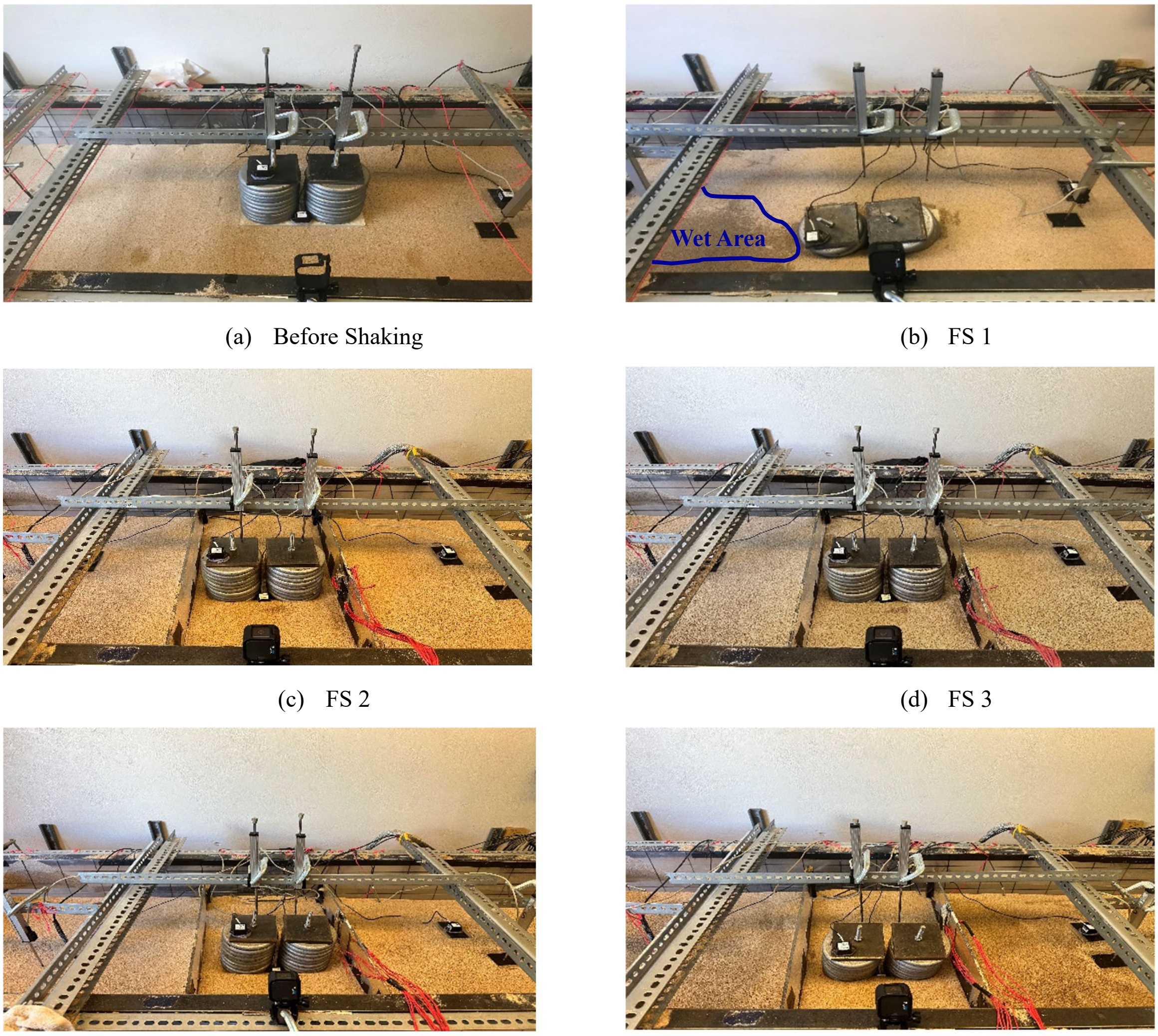


(a) Before Shaking

(b) FS 1

(c) FS 2

(d) FS 3

(e) FS 4

(f) FS 5

**Fig 7** Observed foundation settlement and tilting in a series of tests.

**3.4 Bending moment on sheet piles**

As outlined in Section 2.5, a total of four pairs of strain gauges were utilized to record the time histories of strain. Due to space constraints, detailed strain time histories are not provided in this context. The maximum strain values were computed from the recorded strain time histories, and subsequently, the maximum bending moment exerted on the sheet piles was determined based on these calculated strain values and presented with the variation of the height of the ground model as shown in **Fig. 8**.

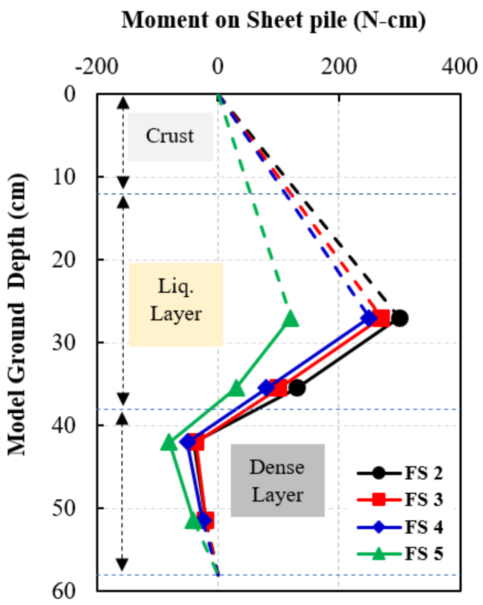


**Fig 8** The variation of longitudinal bending moment with model ground depth.

As depicted in **Fig. 8**, the changes in bending moment highlight that the middle portion of the liquefiable soil layer experienced more substantial magnitudes of bending moment in comparison to the surrounding layers. This phenomenon can be attributed to the lateral displacement of the liquefiable soil layer during shaking, which was obstructed by the presence of the sheet pile, leading to an escalation in the bending moment magnitude. Moreover, it was assumed that the bending moment of the sheet pile decreased linearly to zero from the middle of the liquefiable layer to the surface of the crust. This assumption was based on the sheet pile being unrestricted in movement at the surface of the crust. However, variations could occur due to the potential movement of the crust's surface, resulting in lateral pressure exerted on the sheet pile. This pressure might generate bending moments at the top of the sheet pile In summary, the overall pattern of bending moment variation along the length of the sheet piles exhibited a consistent trend.

As indicated in **Fig. 8**, FS 5 demonstrated a lower bending moment in comparison to the other experiments. This discrepancy can be attributed to the water migration during shaking, resulting in a reduction of the applied lateral pressure on the sheet pile. However, in the case of the PFS with a lower opening in the end-bearing section, a comparable bending moment was observed with full-length sheet piles. This similarity is explained by the fact that even with a reduced opening, the PFS provided sufficient bottom fixity for the sheet pile.

**4. Conclusions**

The objective of this investigation was a comparative analysis of full-length and partial floating end-bearing sheet piles within a model ground, aiming to mitigate liquefaction-induced foundation settlement using a series of 1-g shaking table tests. The following conclusions can be drawn from the test results and discussions.

- The installation of the full-length sheet pile into the ground model changed the EPWP generation into a narrower width and dissipated quickly. However, the gradual increase in partial floating end-bearing sheet piles led to a wider width of EPWP generation, dissipating at a slower rate.
- The reduction in foundation settlement associated with the deployment of PFS, encompassing 75% and 87% of the firm layer, closely approximated the performance of full-length sheet piling.
- The application of PFS allowed for a reduction of 8.7% in sheet piling requirements while closely preserving the level of foundation settlement reduction achieved with full-length sheet piling.
- The maximum bending moment was higher in the middle portion of the liquefied soil layer. The maximum bending moment was reduced because of the water migration through the sheet pile during shaking, resulting in a reduction of the applied lateral pressure on the sheet pile.

**5. Acknowledgements**

This work was supported by funding through the GAANN Fellowship which stands for Graduate Assistance in Areas of National Need, which is a program sponsored by the U.S. Department of Education. Furthermore, the authors thank the staff at the University of Nevada Reno, for their assistance in conducting the test.

**References**

Alam, M. K. et al., 2023. Effect of shaking duration on foundation settlement in liquefiable soils: 1-g shake table tests. In *Geo-Congress 2023*, pp. 89-98.

Ashford, S. A. et al., 2011. Geotechnical quick report on the Kanto plain region during the march 11, 2011, off pacific coast of Tohoku earthquake, Japan. GEER association report no GEER-025a, *Geotechnical Extreme Events Reconnaissance (GEER).*

Bai, Y. et al., 2017. Building damage assessment in the 2015 Gorkha, Nepal, earthquake using only post-event dual polarization synthetic aperture radar imagery. *Earthquake Spectra*, 33(1_suppl), 185-195.

Bray, J. D. & Dashti, S., 2014. Liquefaction-induced building movements. *Bulletin of Earthquake Engineering,* 12, 1129-1156.

Cetin, K. O. et al., 2023. February 6, 2023 Türkiye Earthquakes: Report on geoscience and engineering impacts. GEER Association Report No GEER-82, *Geotechnical Extreme Events Reconnaissance (GEER).*

Fujiwara, K. et al., 2020. Quantitative evaluation of PFS (Partial Floating Sheet-pile) method under liquefaction. *In Geotechnics for Sustainable Infrastructure Development Springer, Singapore,* pp. 467-472.

Fujiwara, K. et al., 2021. 3-D Numerical analysis of partial floating sheet-pile method as countermeasure for liquefaction. *Journal of Japan Society of Civil Engineers (JSCE)*, 9(1), 138-147.

Harata, N. et al., 2008. Countermeasures against settlement of embankment on soft ground with PFS (Partial Floating Sheet-Pile) method. *Proceedings of the 2nd International Workshop held in Glasgow, Scotland*, 3-5 September 2008 (p. 345). CRC Press.

Iai, S., 1989. Similitude for shaking table tests on the soil-structure fluid model in 1g gravitational field. *Journal of Soils and Foundations,* Vol. 29, No. 1: 105-118.

Kasama, K. et al., 2020. Seismic damage investigation for river levees reinforced by steel sheet piling method due to the 2016 Kumamoto earthquake. *In Geotechnics for Sustainable Infrastructure Development Springer, Singapore, pp. 853-858.*

Motamed, R. & Towhata, I., 2010. Mitigation measures for pile groups behind quay walls subjected to lateral flow of liquefied soil: Shake table model tests. *Soil Dynamics and Earthquake Engineering*, 30(10), 1043-1060.

Orang, M. J. et al., 2019. Experimental evaluation of spatial variability effects on liquefaction-induced settlements. In *Geo-Congress 2019: Earthquake Engineering and Soil Dynamics,* 294-303. Reston, VA: American Society of Civil Engineers.

Otani, J., 2021. State of the art report on sheet pile method in geotechnical engineering -development of PFS method. *Proceedings of the second International Conference on Press-in Engineering* 2021, Kochi, Japan, 67-84.

Orang, M. J. et al., 2021. Large-Scale shake table tests on a shallow foundation in liquefiable soils. *Journal of Geotechnical and Geoenvironmental Engineering*, 147(1), 04020152.

Rasouli, R. et al., 2015. Mitigation of seismic settlement of light surface structures by installation of sheet-pile walls around the foundation. *Soil Dynamics and Earthquake Engineering,* 72, pp. 108–118.

Toth, J. & Motamed, R., 2017. Parametric study on liquefaction-induced building settlements using 1-g shake table experiments. The *3rd International Conference on Performance Based Design in Earthquake Geotechnical Engineering, Vancouver*, CA, July 16-19, 2017, Paper no. 149.